Chemical Science

ROYAL SOCIETY OF CHEMISTRY

EDGE ARTICLE

View Article Online
View Journal | View Issue

Check for updates

Cite this: *Chem. Sci.*, 2023, **14**, 10429

All publication charges for this article have been paid for by the Royal Society of Chemistry

Received 15th July 2023
Accepted 28th August 2023

DOI: 10.1039/d3sc03649a

rsc.li/chemical-science

Open Access Article. Published on 13 2566. Downloaded on 12/5/2569 1:38:58.
This article is licensed under a Creative Commons Attribution-NonCommercial 3.0 Unported Licence.

Ionomer degradation in catalyst layers of anion exchange membrane fuel cells†

Qihao Li,[a] Meixue Hu,[b] Chuangxin Ge,[b] Yao Yang,[c] Li Xiao,*[b] Lin Zhuang*[b] and Héctor D. Abruña*[a]

Anion exchange membrane fuel cells (AEMFCs) that operate at high pH, offer the advantage of enabling the use of abundant 3d-transition metal-based electrocatalysts. While they have shown remarkable improvement in performance, their long-term durability remains insufficient for practical applications with the alkaline polymer electrolytes (APEs) being the limiting factor. The stability of APEs is generally evaluated in concentrated alkaline solutions, which overlooks/oversimplifies the complex electrochemical environment of the catalyst layer in membrane electrode assembly (MEA) devices. Herein, we report a study of the degradation of the membrane and ionomer independently under realistic H_2–air (CO_2 free) fuel cell operation, using proton nuclear magnetic resonance (^{1}H-NMR), cyclic voltammetry (CV), electrochemical impedance spectroscopy (EIS), and X-ray photoelectron spectroscopy (XPS). While the membrane degradation was minimal after the AEMFC stability test, the ionomer in the catalyst layers degraded approximately 20% to 30% with the cathode being more severely affected than the anode. The ionomer degradation decreased the catalyst utilization and significantly increased the ionic resistance, leading to significant performance degradation in the AEMFC stability test. These findings emphasize the importance of ionomer stability and the need to consider the electrochemical environments of MEAs when evaluating the stability of APEs.

Introduction

Alkaline polymer electrolyte fuel cells (AEMFCs) have drawn increasing attention in recent years due to their advantage of utilizing nonprecious metals as electrocatalysts, thus enabling large-scale commercialization of fuel cell technologies.[1,2] The development of a key component, the alkaline polymer electrolyte (APE), has been a critical part of AEMFC technology.[3–5] With the development of APEs with high ionic conductivity and mechanical strength, AEMFCs have been able to achieve a high performance of up to 3.4 W cm^{-2},[6–8] which is significantly higher than that of typical proton exchange membrane fuel cells (PEMFCs).[9] Nonprecious metal-based catalysts, such as transition metal oxides and nitrides, have also been investigated and tested and have achieved good fuel cell performance, demonstrating the potential of AEMFC technology.[10–12] However, the long term stability/durability of AEMFCs still remains a significant challenge in realistic membrane electrode assembly (MEA) devices. Most of the reported stabilities lie within the range of several hundred hours or less,[13,14] which is far from the stability target for realistic applications (>8000 h).[15]

The degradation mechanisms of polyelectrolyte fuel cells can be divided into structural failures, including those of the gas diffusion layer, catalyst layer, and interfaces, as well as chemical degradation of the catalysts and polyelectrolytes.[16–18] Great efforts have been devoted to the development of alkaline-stable APEs, including designing heteroatom-free backbones and stable cations such as piperidinium.[6,19–22] However, the stability of APEs still remains a limiting factor in AEMFCs.

The stability of APEs is generally tested in concentrated alkaline solutions at elevated temperatures, which mainly evaluates nucleophilic substitution (S_N2) and elimination (E2) degradation pathways.[23] Since such testing environments are different from those present in fuel cells and do not take into account the complexity of the catalyst layer, many APE degradation pathways that are known to exist in AEMFCs, such as radical attack and oxidation at high potential, cannot be properly evaluated in alkaline solutions.[24–26] As a result, APEs that perform well in alkaline stability tests do not necessarily exhibit comparable fuel cell stability. For example, while quaternary ammonium poly(*N*-methyl-piperidine-co-*p*-terphenyl) (QAPPT) retains over 95% of its cation exchange capacity after a 5000 hour alkaline stability test, its AEMFC stability is limited to only

[a]*Department of Chemistry and Chemical Biology, Cornell University, Ithaca, New York 14853, USA. E-mail: hda1@cornell.edu*

[b]*College of Chemistry and Molecular Sciences, Hubei Key Lab of Electrochemical Power Sources, Wuhan University, Wuhan 430072, PR China. E-mail: chem.lily@whu.edu.cn; lzhuang@whu.edu.cn*

[c]*Department of Chemistry, Miller Institute, University of California, Berkeley, Berkeley, California 94720, USA*

† Electronic supplementary information (ESI) available. See DOI: https://doi.org/10.1039/d3sc03649a

© 2023 The Author(s). Published by the Royal Society of Chemistry

Open Access Article. Published on 13 2566. Downloaded on 12/5/2569 1:38:58.
This article is licensed under a Creative Commons Attribution-NonCommercial 3.0 Unported Licence.

a few hundred hours.[6] This discrepancy highlights the need for detailed studies of the degradation of APEs under AEMFC conditions, particularly the degradation, under electrochemical conditions, of the ionomer present in the catalyst layers.

In this work, we have studied the degradation of the membrane and ionomer separately using proton nuclear magnetic resonance (^{1}H-NMR), electrochemical impedance spectroscopy (EIS), and X-ray photoelectron spectroscopy (XPS). We have found that the degradation in AEMFC performance can be largely attributed to the degradation of the ionomer in the catalyst layer, while the membrane itself exhibited no significant changes. Approximately 20% to 30% of the ionomer's ammonium cations (responsible for ion transport) degraded to tertiary amines, with further degradation to secondary amines being observed, leading to significant performance degradation and to a 4- to 8-fold increase in the ionic resistance of the catalyst layer. These findings emphasize the significance of assessing the stability of APEs under realistic conditions that closely resemble those of the AEMFC environment, and the need to take into account degradation pathways that exist and can be exacerbated in an electrochemical environment.

Results and discussion

An AEMFC utilizing QAPPT as both the membrane and ionomer, in combination with a commercial Pt/C catalyst on both the anode and cathode, was tested at a constant current density of 0.6 A cm^{-2}. Fig. 1a presents the cell voltage and high-frequency resistance (HFR) over a period of 60 hours. The rapid decline in cell voltage observed in the first few hours can be attributed to the previously observed imbalance in water distribution, which leads to an increase in mass transport resistance.[27] This is confirmed by the electrochemical impedance spectra (EIS) obtained in the first 3 hours and the corresponding distribution of relaxation time (DRT) analysis, shown in Fig. S1.† While the reaction resistance showed only a slight increase, the mass transport resistance increased significantly. Afterwards, the cell voltage gradually decreased while the HFR increased. After 40 hours, the HFR increased dramatically, nearly doubling from about 130 to 250 mΩ cm^2, accompanied by a faster decrease in cell voltage. Fig. 1b shows that the fuel cell performance decreased dramatically after the 60 hour stability test. The peak power density (PPD) decreased from 1 to 0.4 W cm^{-2}, and the current density at 0.4 V decreased from 2.5 to 1 A cm^{-2}. The performance decrease remains evident even after *iR* correction, as depicted in Fig. S2.† This suggests that the decline in performance cannot be solely attributed to membrane ionic resistance. The stability of the AEMFC can be extended under milder stability testing conditions. For example, when operated at 70 °C at a current density of 0.2 A cm^{-2}, the cell voltage decreased from around 0.75 V to 0.6 V in 400 hours, and subsequently experienced a rapid decline after 400 hours, showing better stability with a similar degradation trend (see Fig. S3†).

In order to examine any chemical changes in the QAPPT membrane after the stability test, the catalyst layer was first removed from the membrane electrode assembly (MEA) by sonication in a mixture of ethanol and water. The MEA was then dried and dissolved in hexadeuterated dimethyl sulfoxide (DMSO-d_6) to obtain the proton nuclear magnetic resonance (^{1}H-NMR) spectrum. Fig. 2a presents the ^{1}H-NMR spectra before and after the stability test, suggesting no significant changes. The cation grafting ratio (GR) was calculated using the area ratio between piperidinium methyl protons at 3.2 ppm (H_4) and arylene protons at 7.4–7.8 ppm (H_{1-3}) as reported in the literature.[6,28] The GR decreased slightly from 90% to 89%, indicating that membrane degradation is not the main reason accounting for the increase in ionic resistance observed during the stability test. The cyclic voltammograms (CV) of the MEA catalyst layers before and after stability testing are presented in Fig. 2b. One can observe that the features in the hydrogen underpotential deposition (H-UPD) region became less well-defined after the stability test, particularly for the anode. Integration of the charge in the H-UPD region revealed that, after stability testing, the electrochemical surface area (ECSA)

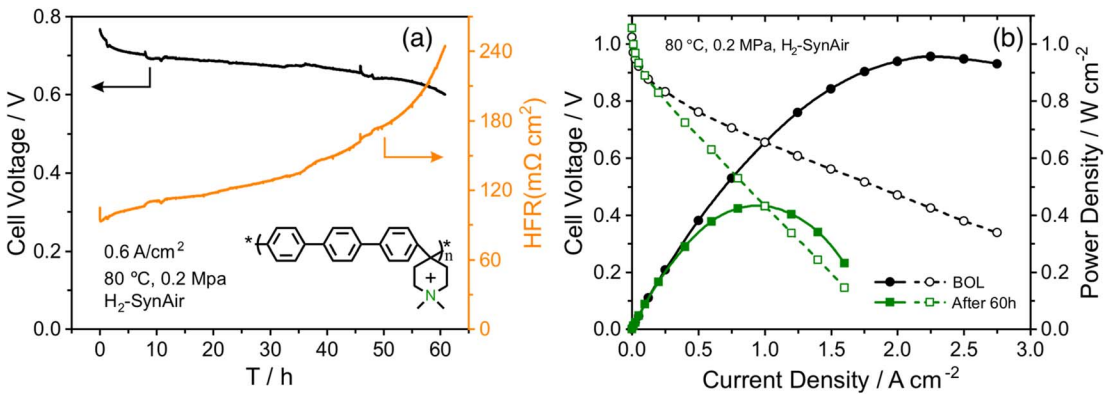

Fig. 1 (a) Fuel cell voltage and high-frequency resistance (HFR) during a stability test at a constant current density of 0.6 A cm^{-2} using quaternary ammonium poly (*N*-methyl-piperidine-co-*p*-terphenyl) (QAPPT) as both the membrane and ionomer. The chemical structure of the QAPPT membrane is depicted in the inset. The cell temperature was set to 80 °C with a back pressure of 0.2 MPa. Hydrogen and CO_2-free air (SynAir) were flowed into the anode and cathode, respectively, at a flow rate of 400 sccm. (b) Corresponding fuel cell performance at the beginning of life (BOL) and after 60 hours of the stability test.

© 2023 The Author(s). Published by the Royal Society of Chemistry

Open Access Article. Published on 13 2566. Downloaded on 12/5/2569 1:38:58.
This article is licensed under a Creative Commons Attribution-NonCommercial 3.0 Unported Licence.

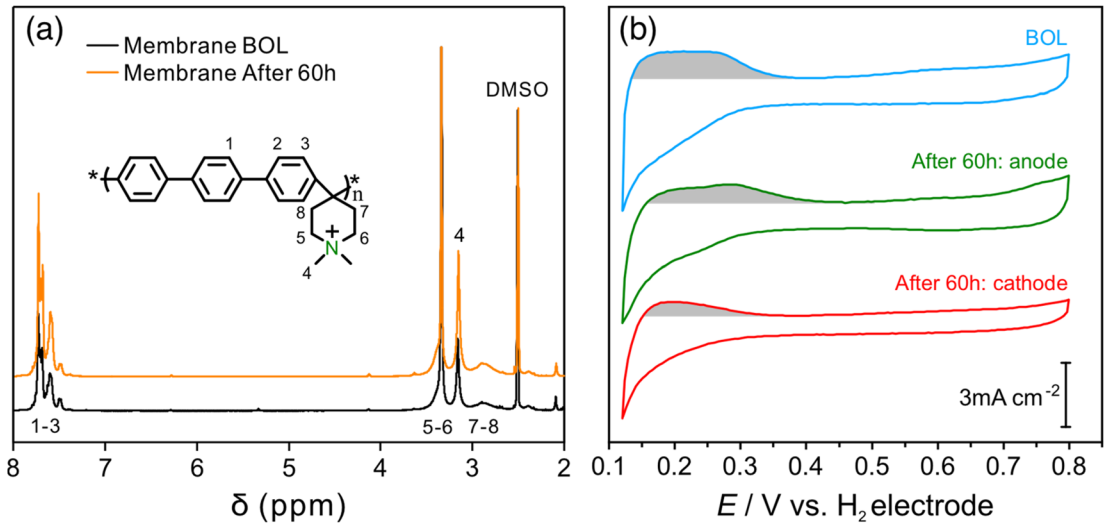

Fig. 2 (a) Proton nuclear magnetic resonance (^{1}H-NMR) spectra of the QAPPT membrane at the BOL and after a 60 hour stability test. (Inset: chemical structure with numbers indicating the peak assignment of the NMR spectra). (b) Cyclic voltammetry (CV) of catalyst layers at the BOL and anode and cathode after 60 hours of stability testing. CV was performed with a 2-electrode configuration with the side purging hydrogen serving as both the reference and counter electrode. Note that the CVs of the anode and cathode were identical at the BOL.

decreased by 24% and 48% for the anode and cathode, respectively. The decrease in ECSA could result from (i) an increase in the Pt particle size or loss of Pt due to dissolution and related processes, with both resulting in a smaller Pt surface area, or (ii) a decrease in the ionic conductivity of the catalyst layer, which would lead to a loss of Pt surface accessibility in the catalyst layer. The X-ray diffraction (XRD) spectra of the catalyst layer displayed no significant peak shift at both the anode and cathode. The average crystallite size, calculated using Scherrer's equation, was determined to be 2.0 nm at the BOL, and 2.1 nm and 2.3 nm for the anode and cathode after 60 hours of the stability test, respectively (Fig. S4†). This minor change is insufficient to account for the alteration in the H-UPD region ECSA. To further analyze the decrease in ECSA, we measured the ionic conductivity in the catalysts layers.

The direct measurement of ionic conductivity in the catalysts layers is challenging since they are electrically conductive, and the complex electrochemical reaction processes of the two electrodes in the MEA further complicate the EIS behavior and interpretation. To mitigate/overcome these challenges, we measured the EIS spectrum under nitrogen with the potential held within the double layer region (0.45 V) to eliminate/minimize the contributions from the electrochemical reaction, while the other electrode was purged with hydrogen so its behavior could be minimized due to the fast hydrogen reaction kinetics. Based on de-Levie's solution for the transmission line model,[29] the impedance $Z_c(f)$ and complex capacitance $C_c(f)$ can be described by using the following equations:

$$Z_c(f) = \frac{R_{ion}}{\sqrt{j2\pi R_{ion} C_{dl} f}} \coth\left(\sqrt{j2\pi R_{ion} C_{dl} f}\right) \quad (1)$$

$$C_c(f) = \frac{1}{j2\pi f Z_c(f)} = \frac{C_{dl}}{\sqrt{j2\pi R_{ion} C_{dl} f}} \tanh\left(\sqrt{j2\pi R_{ion} C_{dl} f}\right) \quad (2)$$

where R_{ion} is the ionic resistance in the catalyst layer, C_{dl} is the double layer capacitance between QAPPT and electrically conductive components, j is the imaginary unit, and f is the frequency. In addition, the catalyst layer ionic transport resistance can be calculated by using the following equation:

$$f_p = 0.404/R_{ion} C_{dl} \quad (3)$$

where f_p is the peak frequency in the real capacitance plot.

The EIS spectrum (Fig. S5†) indicates that the resistance of the membrane increased from 20 to 40 mΩ after the stability test, which partially explains the increase in HFR. The corresponding real and imaginary capacitance plots of the catalyst layer EIS spectrum are shown in Fig. 3a and b. The capacitance of the anode and cathode decreased from 28 mF cm^{-2} to 23 mF cm^{-2} and 20 mF cm^{-2}, respectively, after the stability test. This decrease in capacitance at the ionomer/catalyst interface is consistent with the observed decrease in ECSA following the CV tests. The peak frequency for the anode and cathode decreased from 25 to 6 and 4 Hz, respectively. The ionic resistance of the catalyst layer (R_{ionic}) was calculated and is shown in Fig. 3c, with a significant increase from 0.6 to 2.2 and 6.4 Ω cm^2 for the anode and cathode, respectively. The decrease in ionomer/catalyst interface capacitance and increase in ionic resistance of the catalyst layer is consistent with the observed decrease in ECSA and less well-defined H-UPD features in the CV profiles after the stability test. Collectively, the results of these experiments suggest that the ionomer in the catalyst layer degrades during the stability test, resulting in lower Pt catalyst utilization and an increase in the ionic resistance of the catalyst layer. And all experimental evidence indicates that the extent of degradation is more significant at the cathode. These observations, together with the ^{1}H-NMR results of the membrane after the stability test, lead to the conclusion that there is a significant

Open Access Article. Published on 13 2566. Downloaded on 12/5/2569 1:38:58.
This article is licensed under a Creative Commons Attribution-NonCommercial 3.0 Unported Licence.

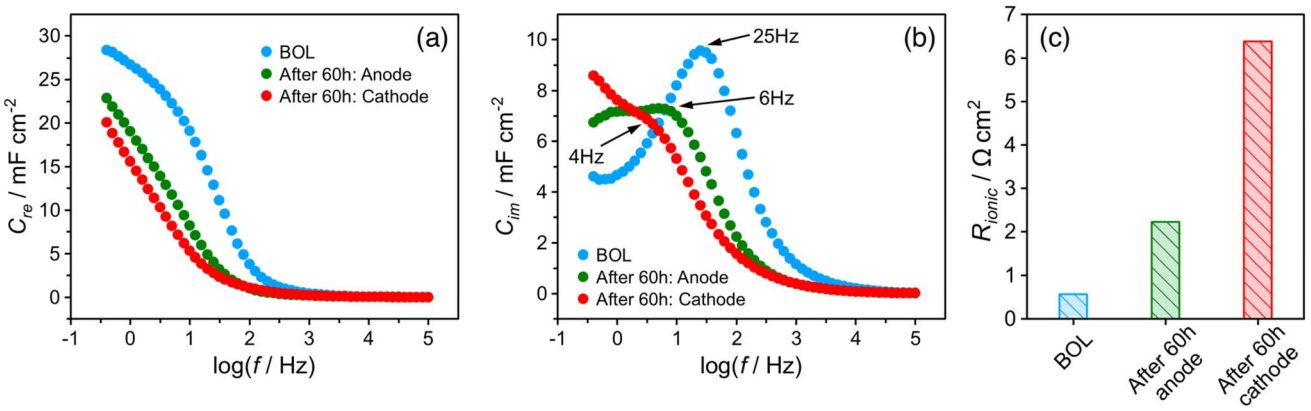

Fig. 3 Experimental (a) real and (b) imaginary capacitance plots of the catalyst layer at the BOL, anode, and cathode after a 60 hour stability test. (c) Corresponding calculated ionic resistance in the catalyst layer.

difference in the degradation rate between the membrane and the catalyst layer ionomer, which is more pronounced at the cathode.

To further study the changes in the ionomer, especially the ammonium cation, the X-ray photoelectron spectroscopy (XPS) spectrum of the catalyst layer was recorded before and after the stability test. Fig. 4a shows the N 1s XPS spectra of the catalyst layer before the stability test. The peaks with binding energies of around 402.7 eV and 399.2 eV can be assigned to quaternary amine (ammonium cation) and tertiary amine, respectively,[30] with 94% being quaternary amine and 6% being tertiary amine, which is in close agreement with the 95% cation grafting ratio (GR) of the QAPPT used as an ionomer in the catalyst layer. Fig. 4b and c show the N 1s XPS spectrum of the anode and cathode after the 60 hour stability test, respectively. They show that the percentage of quaternary ammonium decreased to 73% and 63% for the anode and cathode, respectively, indicating a 21% and 31% degradation of the ammonium cations. This explains the capacitance decrease and ionic resistance increase in the catalyst layer, which causes the decrease in performance after the stability test. It is also in agreement with a lower ECSA and higher ionic resistance observed in the cathode when compared with the anode. Furthermore, a peak with a binding energy of around 397.7 eV emerged in the N 1s XPS spectrum after the stability test in both the anode and cathode, with 7% and 15% relative intensity, respectively, which can be assigned to secondary amines.[30] Structures of initial quaternary ammonium and subsequent tertiary and secondary amines based on likely degradation pathways are shown in Fig. 4d. Nucleophilic substitution (S_N2) and elimination (E2) degradations are the most commonly reported chemical pathways. In addition, oxidative radical induced electrophilic degradations are also possible because of piperidinium's lability to electrophilic attack. Alternative techniques are required in future studies to reveal the degradation mechanism in detail.

Reported degradation products of quaternary ammoniums in APE alkaline stability tests include tertiary amines[23,28,31,32] The further degradation of tertiary amines into secondary amines in

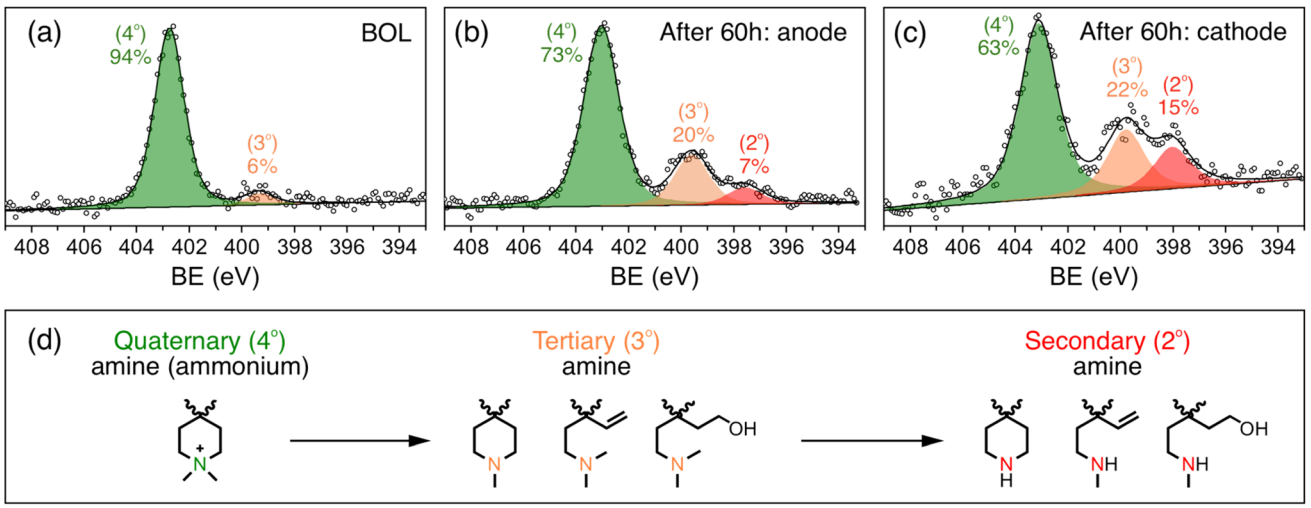

Fig. 4 N 1s XPS spectra of the catalyst layer at (a) the beginning of life (BOL) and the (b) anode and (c) cathode after 60 hours of stability testing. (d) Quaternary and possible tertiary and secondary amine structures corresponding to N 1s XPS peaks.

© 2023 The Author(s). Published by the Royal Society of Chemistry

Open Access Article. Published on 13 2566. Downloaded on 12/5/2569 1:38:58.
This article is licensed under a Creative Commons Attribution-NonCommercial 3.0 Unported Licence.

the catalyst layers highlights the amplifying impact of the electrochemical environment on the degradation of the alkaline polymer electrolyte, particularly the cations. The severe degradation of the ionomer in contrast to the almost unchanged membrane after the stability test also highlights the necessity of considering the effect of electrochemical environment in MEAs on the degree and pathways of APE degradation. Possible reasons for this difference are (1) the applied potential and (2) radicals generated during electrochemical reactions in the catalyst layer. This can also explain the higher degree of ionomer degradation in the cathode, which may be attributed to its higher potential and greater generation of radicals during the oxygen reduction reaction. These results unambiguously highlight the significance of ionomer stability and the need to evaluate the stability of APEs while considering the influence of the electrochemical environments. Studying the influence of potential, radicals and electrochemical reactions on ionomer stability is currently underway.

Conclusions

In this study, we investigated the degradation of both the membrane and catalyst layer, independently, using ^{1}H-NMR, CV, and EIS, after subjecting AEMFCs to constant current stability tests. We observed that while the membrane remained virtually unchanged, the ionic resistance in the catalyst layers significantly increased and the ECSA decreased, with the cathode being more significantly affected than the anode. N 1s XPS analysis revealed that the quaternary amine of the ionomer in the catalyst layer degraded by 20–30%, which is the main reason for AEMFC degradation using QAPPT. Our findings underscore the critical role of ionomer stability in AEMFCs and highlight the influence of the catalyst layer environment on the degradation rates and pathways of APEs. This suggests that future research should consider the complex electrochemical environment, including the applied potential and generation of radicals, when evaluating APEs' stability.

Data availability

All study data are included in the article and/or ESI.†

Author contributions

Q. L. conceived and designed the experiments, wrote the manuscript under the supervision of L. X., L. Z., and H. D., and conducted AEMFC, EIS, and electrochemical tests and analysis. M. H. synthesized the QAPPT membrane, conducted 1H-NMR tests and analysis. C. G. and Y. Y. contributed to the results analysis and discussion. All authors participated in manuscript review.

Conflicts of interest

The authors declare no competing financial interest.

Acknowledgements

This research was primarily supported by the National Natural Science Foundation of China (NSFC) grants 21991154, 21991150, and 22122204, and the Fundamental Research Funds for the Central Universities 885 grant 2042022kf1174. L. Q. acknowledges support by the New York State Energy Research and Development Authority 873 (NYSERDA) under agreement 146218 and the Center for Alkaline Based Energy Solutions (CABES) funded by the U.S. Department of Energy (DOE), Office of Science, Basic Energy Sciences (BES), under award DE-SC0019445.

References

1 S. Lu, J. Pan, A. Huang, L. Zhuang and J. Lu, Alkaline polymer electrolyte fuel cells completely free from noble metal catalysts, *Proc. Natl. Acad. Sci. U.S.A.*, 2008, **105**, 20611–20614.

2 Y. Yang, C. R. Peltier, R. Zeng, R. Schimmenti, Q. Li, X. Huang, Z. Yan, G. Potsi, R. Selhorst, X. Lu, W. Xu, M. Tader, A. V. Soudackov, H. Zhang, M. Krumov, E. Murray, P. Xu, J. Hitt, L. Xu, H. Y. Ko, B. G. Ernst, C. Bundschu, A. Luo, D. Markovich, M. Hu, C. He, H. Wang, J. Fang, R. A. DiStasio Jr., L. F. Kourkoutis, A. Singer, K. J. T. Noonan, L. Xiao, L. Zhuang, B. S. Pivovar, P. Zelenay, E. Herrero, J. M. Feliu, J. Suntivich, E. P. Giannelis, S. Hammes-Schiffer, T. Arias, M. Mavrikakis, T. E. Mallouk, J. D. Brock, D. A. Muller, F. J. DiSalvo, G. W. Coates and H. D. Abruna, Electrocatalysis in Alkaline Media and Alkaline Membrane-Based Energy Technologies, *Chem. Rev.*, 2022, **122**, 6117–6321.

3 S. Noh, J. Y. Jeon, S. Adhikari, Y. S. Kim and C. Bae, Molecular Engineering of Hydroxide Conducting Polymers for Anion Exchange Membranes in Electrochemical Energy Conversion Technology, *Acc. Chem. Res.*, 2019, **52**, 2745–2755.

4 J. Pan, C. Chen, L. Zhuang and J. Lu, Designing advanced alkaline polymer electrolytes for fuel cell applications, *Acc. Chem. Res.*, 2011, **45**, 473–481.

5 J. R. Varcoe, P. Atanassov, D. R. Dekel, A. M. Herring, M. A. Hickner, P. A. Kohl, A. R. Kucernak, W. E. Mustain, K. Nijmeijer, K. Scott, T. Xu and L. Zhuang, Anion-exchange membranes in electrochemical energy systems, *Energy Environ. Sci.*, 2014, **7**, 3135–3191.

6 H. Peng, Q. Li, M. Hu, L. Xiao, J. Lu and L. Zhuang, Alkaline polymer electrolyte fuel cells stably working at 80 °C, *J. Power Sources*, 2018, **390**, 165–167.

7 G. Huang, M. Mandal, X. Peng, A. C. Yang-Neyerlin, B. S. Pivovar, W. E. Mustain and P. A. Kohl, Composite Poly(norbornene) Anion Conducting Membranes for Achieving Durability, Water Management and High Power (3.4 W cm^{-2}) in Hydrogen/Oxygen Alkaline Fuel Cells, *J. Electrochem. Soc.*, 2019, **166**, F637–F644.

8 Q. Li, H. Peng, Y. Wang, L. Xiao, J. Lu and L. Zhuang, The Comparability of Pt to Pt–Ru in Catalyzing the Hydrogen Oxidation Reaction for Alkaline Polymer Electrolyte Fuel

Open Access Article. Published on 13 2566. Downloaded on 12/5/2569 1:38:58.
This article is licensed under a Creative Commons Attribution-NonCommercial 3.0 Unported Licence.

Cells Operated at 80 °C, *Angew. Chem., Int. Ed.*, 2018, **58**, 1456–1460.
9 C.-Y. Liu and C.-C. Sung, A review of the performance and analysis of proton exchange membrane fuel cell membrane electrode assemblies, *J. Power Sources*, 2012, **220**, 348–353.
10 Y. Wang, Y. Yang, S. Jia, X. Wang, K. Lyu, Y. Peng, H. Zheng, X. Wei, H. Ren, L. Xiao, J. Wang, D. A. Muller, H. D. Abruna, B. J. Hwang, J. Lu and L. Zhuang, Synergistic Mn–Co catalyst outperforms Pt on high-rate oxygen reduction for alkaline polymer electrolyte fuel cells, *Nat. Commun.*, 2019, **10**, 1506.
11 Y. Yang, H. Peng, Y. Xiong, Q. Li, J. Lu, L. Xiao, F. J. DiSalvo, L. Zhuang and H. D. Abruña, High-Loading Composition-Tolerant Co–Mn Spinel Oxides with Performance beyond 1 W cm^{-2} in Alkaline Polymer Electrolyte Fuel Cells, *ACS Energy Lett.*, 2019, **4**, 1251–1257.
12 C. Ge, Q. Li, M. Hu, G. Wang, L. Xiao, J. Lu and L. Zhuang, Application of rock-salt-type Co–Mn oxides for alkaline polymer electrolyte fuel cells, *J. Power Sources*, 2022, **520**, 230868.
13 D. R. Dekel, Review of cell performance in anion exchange membrane fuel cells, *J. Power Sources*, 2018, **375**, 158–169.
14 W. E. Mustain, M. Chatenet, M. Page and Y. S. Kim, Durability challenges of anion exchange membrane fuel cells, *Energy Environ. Sci.*, 2020, **13**, 2805–2838.
15 *DOE Technical Targets for Fuel Cell Systems and Stacks for Transportation Applications*, **https://www.energy.gov/eere/fuelcells/doe-technical-targets-fuel-cell-systems-and-stacks-transportation-applications**, (accessed 04/12/2023).
16 R. Borup, J. Meyers, B. Pivovar, Y. S. Kim, R. Mukundan, N. Garland, D. Myers, M. Wilson, F. Garzon and D. Wood, Scientific aspects of polymer electrolyte fuel cell durability and degradation, *Chem. Rev.*, 2007, **107**, 3904–3951.
17 S. Holdcroft, Fuel Cell Catalyst Layers: A Polymer Science Perspective, *Chem. Mater.*, 2014, **26**, 381–393.
18 L. Dubau, L. Castanheira, F. Maillard, M. Chatenet, O. Lottin, G. Maranzana, J. Dillet, A. Lamibrac, J.-C. Perrin, E. Moukheiber, A. ElKaddouri, G. De Moor, C. Bas, L. Flandin and N. Caqué, A review of PEM fuel cell durability: materials degradation, local heterogeneities of aging and possible mitigation strategies, *Wiley Interdiscip. Rev.: Energy Environ.*, 2014, **3**, 540–560.
19 T. H. Pham, J. S. Olsson and P. Jannasch, Effects of the *N*-alicyclic cation and backbone structures on the performance of poly(terphenyl)-based hydroxide exchange membranes, *J. Mater. Chem. A*, 2019, **7**, 15895–15906.
20 J. Wang, Y. Zhao, B. P. Setzler, S. Rojas-Carbonell, C. Ben Yehuda, A. Amel, M. Page, L. Wang, K. Hu, L. Shi, S. Gottesfeld, B. Xu and Y. Yan, Poly(aryl piperidinium) membranes and ionomers for hydroxide exchange membrane fuel cells, *Nat. Energy*, 2019, **4**, 392–398.
21 M. Mandal, G. Huang, N. U. Hassan, W. E. Mustain and P. A. Kohl, Poly(norbornene) anion conductive membranes: homopolymer, block copolymer and random copolymer properties and performance, *J. Mater. Chem. A*, 2020, **8**, 17568–17578.
22 J. S. Olsson, T. H. Pham and P. Jannasch, Functionalizing Polystyrene with *N*-Alicyclic Piperidine-Based Cations via Friedel–Crafts Alkylation for Highly Alkali-Stable Anion-Exchange Membranes, *Macromolecules*, 2020, **53**, 4722–4732.
23 M. G. Marino and K. D. Kreuer, Alkaline stability of quaternary ammonium cations for alkaline fuel cell membranes and ionic liquids, *ChemSusChem*, 2015, **8**, 513–523.
24 K. M. Hugar, W. You and G. W. Coates, Protocol for the Quantitative Assessment of Organic Cation Stability for Polymer Electrolytes, *ACS Energy Lett.*, 2019, **4**, 1681–1686.
25 S. Wierzbicki, J. C. Douglin, A. Kostuch, D. R. Dekel and K. Kruczala, Are Radicals Formed During Anion-Exchange Membrane Fuel Cell Operation?, *J. Phys. Chem. Lett.*, 2020, **11**, 7630–7636.
26 S. Maurya, A. S. Lee, D. Li, E. J. Park, D. P. Leonard, S. Noh, C. Bae and Y. S. Kim, On the origin of permanent performance loss of anion exchange membrane fuel cells: electrochemical oxidation of phenyl group, *J. Power Sources*, 2019, **436**, 226866.
27 M. Hu, Q. Li, H. Peng, H. Ma, L. Xiao, G. Wang, J. Lu and L. Zhuang, Alkaline polymer electrolyte fuel cells without anode humidification and H_2 emission, *J. Power Sources*, 2020, **472**, 228471.
28 J. S. Olsson, T. H. Pham and P. Jannasch, Poly(arylene piperidinium) Hydroxide Ion Exchange Membranes: Synthesis, Alkaline Stability, and Conductivity, *Adv. Funct. Mater.*, 2018, **28**, 1702758.
29 J. H. Jang, S. Jeon, J. H. Cho, S.-K. Kim, S.-Y. Lee, E. Cho, H.-J. Kim, J. Han and T.-H. Lim, Complex Capacitance Analysis of Ionic Resistance and Interfacial Capacitance in PEMFC and DMFC Catalyst Layers, *J. Electrochem. Soc.*, 2009, **156**, B1293–B1300.
30 C. Lei, K. Yang, G. Wang, G. Wang, J. Lu, L. Xiao and L. Zhuang, Impact of Catalyst Reconstruction on the Durability of Anion Exchange Membrane Water Electrolysis, *ACS Sustain. Chem. Eng.*, 2022, **10**, 16725–16733.
31 R. Espiritu, B. T. Golding, K. Scott and M. Mamlouk, Degradation of radiation grafted hydroxide anion exchange membrane immersed in neutral pH: removal of vinylbenzyl trimethylammonium hydroxide due to oxidation, *J. Mater. Chem. A*, 2017, **5**, 1248–1267.
32 A. D. Mohanty, S. E. Tignor, M. R. Sturgeon, H. Long, B. S. Pivovar and C. Bae, Thermochemical Stability Study of Alkyl-Tethered Quaternary Ammonium Cations for Anion Exchange Membrane Fuel Cells, *J. Electrochem. Soc.*, 2017, **164**, F1279–F1285.

© 2023 The Author(s). Published by the Royal Society of Chemistry